Currents and Voltages Induced During Earth Faults in a System Consisting of a Transmission Line and a Parallel Pipeline

K. J. Satsios, D. P. Labridis, P. S. Dokopoulos

Abstract

A numerical procedure employing the finite-element method (FEM) is used in conjunction with Faraday's law, in order to predict the current in a faulted transmission line as well as the induced voltages across points on a pipeline running parallel to the faulted line and remote earth. The problem is a two-dimensional one, because the phase-to-ground fault is assumed to be outside of the parallel exposure so that the conductive interference is negligible. Therefore a two-dimensional finite-element mesh has been solved, that leads to the field distribution and finally to the induced voltages. The effect of the problem "operational parameters" (mitigation wires number, earth resistivity and overhead transmission line geometrical configuration) has been taken into account. The results lead to conclusions that may be useful to power-system engineers.

1 Introduction

The proximity of electric power lines and metal pipelines transporting fluids has become more and more frequent, owing to their having been assigned a common course and to the continual increase in energy consumption. This leads to a stronger power-line interference on pipelines, in view of the increase of fault currents linked to electric network development. An insulated pipeline, even below ground, which follows an electrical line or cable over a certain distance is subjected to significant voltages, especially in cases of earth faults.

AC interference in a pipeline sharing a corridor with a power line consists of an inductive component and a conductive component. Inductive interference, which is occurred by the magnetic field generated by the power line, is present during both normal load conditions and fault conditions on the power line. Conductive interference arises when a power-line structure injects a large magnitude current into the earth during a single-phase-to-ground fault and the pipeline is located near the faulted structure.

Using initially the widely-known *Carson*'s relations [1], various formulae have been proposed [2–5] to study the above interferences. The introduction of computers in the next decade has brought a considerable improvement to the procedures for calculating voltages appearing along an influence area, leading to advanced analytical models [6]. Technical Recommendation No. 7 [6] takes all new knowledge, both theoretically and experimentally derived, into account and represents the present state of the art. On the basis of particular examples it is possible to specify interference caused by earth-fault currents in high-voltage systems or by load currents.

Recently, two extensive research projects introduced practical analytical expressions which could be programmed on hand-held calculators [7] and computerized techniques [8], for the analysis of power-load current inductive coupling to gas pipelines. Furthermore the Electrical Power Research Institute (EPRI) and the American Gas Association (AGA) in a joint research developed the Electromagnetic & Conductive Coupling Analysis from Powerlines to Pipelines (ECCAPP) program [9–11]. Equivalent circuits with concentrated or distributed elements are used in ECCAPP and the self and mutual impedances are calculated using formulae from *Carson* [1], *Pollaczeck* [12] and *Sunde* [5]. In 1987, Study Committee 36 – Interference – of the Cigré conducted an international survey on the problems of proximity of HV power structures to metal pipelines, with emphasis on regulations governing their exposure. The results obtained were published in [13].

More recently (1992), a general document [14–17] entitled "Guide Concerning Influence of High Voltage AC power Systems on Metallic Pipelines" covering problems of influence of HV power structures on metal pipelines has been elaborated within the Cigré Working Group 36.02. This guide has several different objectives:

- Presentation of different influences and problems which result from them.
- Description of simple methods for calculating influences, as well as methods of measurement.
- Presentation of the principal means of reducing influences and description of protection systems.

The authors of this paper believe that a finite-element solution of *Maxwell*'s equations which describe the corresponding electromagnetic field problem may lead to useful conclusions, complementary to already proposed methods. In order to determine both inductive and conductive interferences, a three-dimensional FEM analysis is required. However, in the present work, the two-dimensional electromagnetic field problem of a

faulted overhead transmission line in the presence of buried conductors has been numerically solved with the help of FEM, because the fault is assumed to be outside of the parallel exposure and therefore the conductive interference is negligible.

2 Problem Description

The system under investigation, shown in **Fig. 1** and **2**, consists of a 25 km long corridor shared between one pipeline and one transmission line. A phase-to-earth fault is assumed on the transmission line at point B, which is outside of the parallel exposure. Therefore conductive interference becomes negligible and the present work analyses the inductive coupling between overhead power transmission lines and neighbouring gas pipelines or other conductors, when they run parallel to a line section. Currents are induced in the faulted conductor, skywires and earth. End effects are neglected, i. e. a two-dimensional problem is considered consisting of infinite length conductors. This is reasonable for the lengths of parallel exposure between transmission lines and buried conductors, as encountered in practical applications. The fault is assumed to be in a steady-state condition with 50 Hz nominal frequency.

Concerning the material properties, the earth is assumed to be homogeneous with a varying resistivity corresponding to wet, dry and rocky grounds, respectively. Homogeneity is not a restriction for the program developed, which is capable to solve for a multi-layer earth, or earths with properties varying in the two dimensions (x, y). Pipeline's metal and skywires have conductivities $\sigma_m = \sigma_{sk} = 7 \cdot 10^6$ S/m and relative permeabilities $\mu_{r,m} = \mu_{r,sk} = 250$, respectively. Pipeline's coating has a relative permeability $\mu_{r,c} = 1$ and is assumed to be perfect, which is reasonable for nowadays synthetic coatings [16]. Therefore, the coating conductivity σ_c is assumed to be zero and the corresponding leakage currents

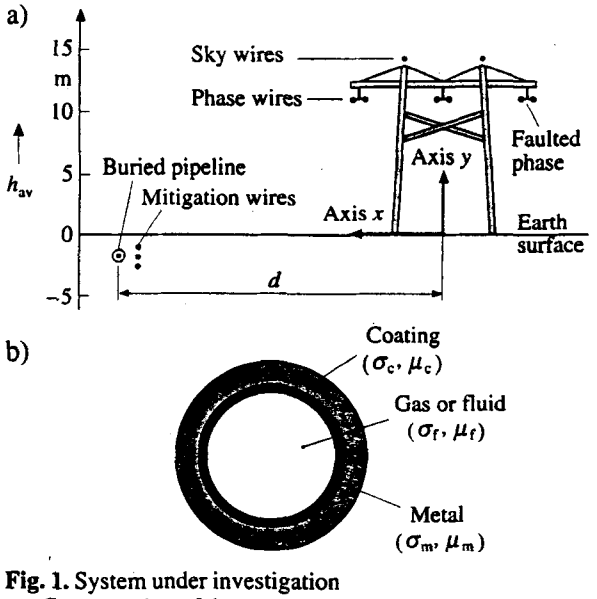

Fig. 1. System under investigation
a) Cross-section of the system
b) Detailed pipeline cross-section

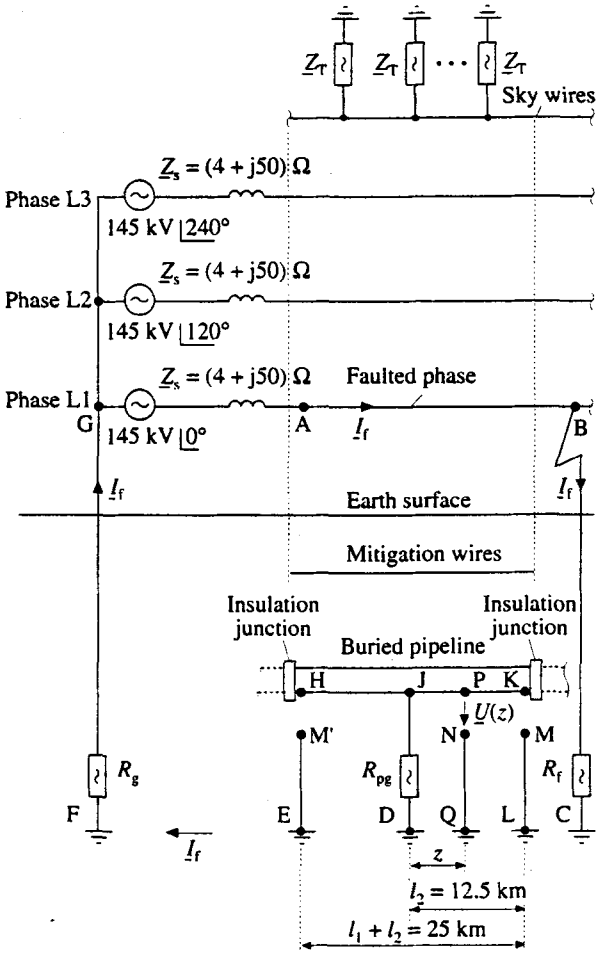

Fig. 2. Circuit diagram of the system under investigation

through the pipeline's coating are neglected. Copper or aluminium mitigation wires shown in Fig. 1a are bare.

The geometry of the transmission line consists of a pair of HAWK ACSR conductors. Skywire conductors radius is 4 mm, pipeline inner radius is 0.195 m, its outer radius is 0.2 m and coating thickness is 0.1 m. The source phase voltage of the terminal is 145 kV behind an impedance of $Z_s = 4.0 + j\,50.0\ \Omega$. The neutral of the source has a ground resistance of $R_g = 0.2\ \Omega$. Tower's ground resistances are negligible and the fault resistance R_f is assumed equal to 20 Ω.

Junctions isolate the pipeline at both ends H and K (shown in **Fig. 2** and **3**) for cathodic protection purposes, and the nearest grounding of pipeline at point J lies 12.5 km away from each insulation junction. Assuming $\sigma_c = 0$ for nowadays synthetic coatings, the total current in the pipeline sections between the insulation junctions and the grounding is zero. However, a voltage will appear across points on both of these sections HJ and KJ, and remote earth. The magnitude of this voltage at a point P is a function of its distance z from the grounding of the pipeline.

The fault current I_f in the power line conductors, which is influenced by the presence of the pipeline, is calculated using FEM results and *Faraday*'s law. Therefore, the required input data for our method are power line and pipeline geometrical configuration, conductors and pipeline physical characteristics, air and earth char-

acteristics, power system terminal parameters (such as source voltages and equivalent source impedances) as well as fault parameters describing fault location and type. The output data are the fault current in the faulty phase conductor, magnetic vector potential (MVP) distribution in the cross-section of the parallel exposure, eddy currents induced in skywires and earth, and voltages induced at points across pipeline sections HJ and KJ and remote earth.

3 Finite-Element Formulation of the Electromagnetic Field

If the cross-section shown in Fig. 1a lies on the x-y plane, the linear two-dimensional electromagnetic diffusion problem for the z-direction components $\underline{A}_z$ and $\underline{J}_z$ of the MVP vector and of the total current density vector, respectively, is described by the system of equations [18]:

$$\frac{1}{\mu_0 \mu_r}\left[\frac{\partial^2 \underline{A}_z}{\partial x^2}+\frac{\partial^2 \underline{A}_z}{\partial y^2}\right]-\mathrm{j}\omega\sigma \underline{A}_z+\underline{J}_z=0, \tag{1a}$$

$$-\mathrm{j}\omega\sigma \underline{A}_z+\underline{J}_{sz}=\underline{J}_z, \tag{1b}$$

$$\iint_{S_i} \underline{J}_z \,\mathrm{d}s=\underline{I}_i, \tag{1c}$$

where σ is the conductivity, ω is the angular frequency, μ_0 and μ_r are the vacuum and relative permeabilities, respectively, $\underline{J}_{sz}$ is the source current density in the z-direction and $\underline{I}_i$ is the current flowing through conductor i of cross-section $\underline{S}_i$.

The FEM formulation of eqs. (1a) to (1c) leads [19] to a matrix equation, which is solved using the *Crout* variation of *Gauss* elimination. From the solution of this system, the values of the MVP in every node of the discretization domain as well as the unknown source current densities are calculated. Consequently, the eddy current density $\underline{J}^e_{ez}$ of element e is obtained from the relation [18]

$$\underline{J}^e_{ez}(x,y)=-\mathrm{j}\omega\sigma \underline{A}^e_z(x,y), \tag{2a}$$

and the total element current density $\underline{J}^e_z$ will be the sum of the conductor-i source current density $\underline{J}_{szi}$ and of the element eddy current density $\underline{J}^e_{ez}$ given by eq. (2a), i. e.

$$\underline{J}^e_z(x,y)=\underline{J}^e_{ez}(x,y)+\underline{J}_{szi}. \tag{2b}$$

Integration of eq. (2b) over a conductor cross-section will give the total current flowing through this conductor.

The total solution domain for our problem, which is a square with 10 km side, is subdivided in first-order triangular finite elements. A *Delaunay*-based [20] adaptive mesh generation algorithm has been used for the original discretization. The continuity requirement of the flux density $\boldsymbol{B}$ on the interface between neighbouring elements has been chosen [21] as the criterion for an iteratively adaptive mesh refinement. The *Delaunay*-based original mesh of approximately 3000 elements, using the above criterion, led in almost all cases tested to a mesh of 14000 to 16000 elements. Relative element distribution in this mesh reveals the good behaviour of the criterion chosen. A subsequent refinement is not necessary because, although it rises the number of triangles up to 50 %, MVP results are hardly influenced.

4 Analysis of Currents and Voltages

The voltage $\underline{U}_{AB}$ across two points A, B is defined from the electrical field $\boldsymbol{E}$ and the path joining A and B as:

$$\underline{U}_{AB}=\int_A^B \boldsymbol{E}\,\mathrm{d}\boldsymbol{l}. \tag{3}$$

This voltage depends not only on the end points A and B, but also on the path, because the field is time-varying. In Fig. 2 and 3 this path is assumed to be a straight line joining A and B.

If displacement currents are neglected, path AB is parallel to the direction of the current density and belongs on the surface of a conductor having conductivity σ, then eq. (3) leads to

$$\underline{U}_{AB}=\int_A^B \boldsymbol{E}\,\mathrm{d}\boldsymbol{l}=\frac{\underline{J}_z\, l}{\sigma}, \tag{4}$$

where $\underline{J}_z$, σ, l are the z-direction component of the total current density, the conductivity and the conductor length, respectively.

The voltage $\underline{U}_{BC}$ across a path BC, e. g. from B to the remote earth C of **Fig. 3**, through which a current $\underline{I}_f$ flows, is given by

$$\underline{U}_{BC}=\int_B^C \boldsymbol{E}\,\mathrm{d}\boldsymbol{l}=\underline{J}_f R_f, \tag{5}$$

where R_f is the fault resistance.

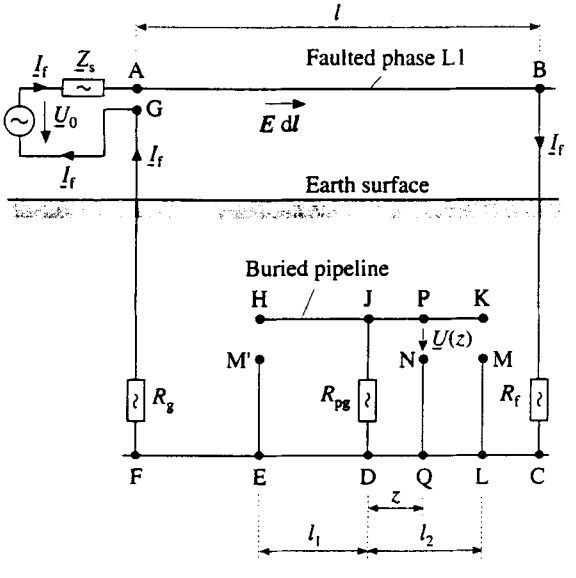

Fig. 3. Circuit diagram of the model shown in Fig. 1 and 2, shown only the faulted phase; this circuit diagram is used for the calculation of fault current $\underline{I}_f$ and of voltage across point P on the pipeline and remote earth N

4.1 Faraday's Law Application for Fault-Current Determination

The earth fault shown in Fig. 2 and 3 leads to a total current $\underline{I}_f$ flowing in the section AB of faulted phase L1 and back along the path ABCLDEFGA. If reference earth CLDEF is supposed to be a conducting plane of infinite conductivity, then current $\underline{I}_f$ *may* be determined by combining FEM calculations and Faraday's law applied in the closed path ABCFGA

$$\oint \boldsymbol{E}\mathrm{d}\boldsymbol{l} + \frac{\partial \Phi}{\partial t} = 0, \tag{6}$$

where Φ is the flux of the magnetic field through the closed path ABCFGA. Using phasors, in a two-dimensional field this flux is given in the plane (x, y) by

$$\underline{\Phi} = \underline{A}_z l, \tag{7}$$

where $\underline{A}_z$ is the z-component of the MVP and l is the length of the path AB.

Using eq. (6) with phasors instead of time functions we obtain

$$\underline{U}_{AB} + \underline{U}_{BC} + \underline{U}_{CF} + \underline{U}_{FG} + \underline{U}_{GA} + \mathrm{j}\omega\underline{\Phi} = 0, \tag{8}$$

where

$$\underline{U}_{AB} = \int_A^B \boldsymbol{E}\mathrm{d}\boldsymbol{l} = \frac{\underline{J}_z l}{\sigma}, \tag{9a}$$

$$\underline{U}_{BC} = \underline{I}_f R_f, \tag{9b}$$

$$\underline{U}_{CF} = 0, \tag{9c}$$

$$\underline{U}_{FG} = \underline{I}_f R_g, \tag{9d}$$

$$\underline{U}_{GA} = -\underline{U}_0 + \underline{I}_f \underline{Z}_s. \tag{9e}$$

Finally, the source phase voltage $\underline{U}_0$ can be expressed with two additive terms in brackets as follows:

$$\underline{U}_0 = \underline{I}_f\left(R_g + \underline{Z}_s + R_f\right) + \left(\frac{\underline{J}_z l}{\sigma} + \mathrm{j}\underline{A}_z \omega l\right). \tag{10}$$

The first term on the right-hand side of eq. (10) is the voltage due to the concentrated elements R_g, $\underline{Z}_s$ and R_f. The second term contains quantities $\underline{J}_z$ and $\underline{A}_z$, which are uniquely determined by FEM calculations for a given fault current $\underline{I}_f$. So, if we impose a current $\underline{I}_{fb} = 1\ \mathrm{A} < 0°$, a base voltage $\underline{U}_b$ is computed from eq. (10) as

$$\underline{U}_b = \underline{I}_{fb}\left(R_g + \underline{Z}_s + R_f\right) + \left(\frac{\underline{J}_{zb} l}{\sigma} + \mathrm{j}\underline{A}_{zb}\omega l\right), \tag{11a}$$

where $\underline{J}_{zb}$ and $\underline{A}_{zb}$ are the current density and the MVP on the surface of the phase conductors, respectively, calculated using FEM. Finally, $\underline{I}_f$ is calculated from

$$\underline{I}_f = \frac{\underline{U}_0}{\underline{U}_b}\underline{I}_{fb}, \tag{11b}$$

where $\underline{U}_0$ is the known source phase voltage of the terminal, shown in Fig. 2 and 3.

The calculation of $\underline{I}_f$ in eqs. (11a) and (11b) takes into account soil properties and buried conductors. It has been checked with results from *Carson*'s [1] relations in simplified cases (i. e. without buried conductors) and the differences found were less than 2 %.

4.2 Faraday's Law Application for Pipeline Voltage Determination

We consider now the pipeline HK of Fig. 2 and 3, running parallel to the faulted phase L1. The pipeline is grounded with a resistance R_{pg} at the point J, while both end-points K and H have no connections to earth, i. e. they correspond to insulating junctions. Applying Faraday's law in the loop PNQDJP, the voltage across a point P and remote earth N is obtained as a function of its distance z from J:

$$\underline{U}_{PN} = \mathrm{j}\underline{A}_z \omega z. \tag{12}$$

The maximum value of this voltage is occurred across point K and remote earth M as:

$$\underline{U}_{KM} = \mathrm{j}\underline{A}_z \omega l_2. \tag{13}$$

Due to the symmetry of pipeline HK across grounding point J, the same conclusions hold for both sections KJ and HJ.

The above method can also be used for other pipeline's configurations, if for example the pipeline is grounded with resistances R_{pg} at both ends – points K and H as shown in **Fig. 4**. In this case section HK is part of the closed loop HKLQDEH and a current $\underline{I}_c$ will flow through it. Applying as previously *Faraday*'s law eq. (6) in the two loops PKLQNP, HKLQDEH, the voltage across a point P, lying between the grounding points H, K, and remote earth N is obtained as:

$$\underline{U}_{PN} = R_{pg}\underline{I}_c\left(\frac{2z}{l_1 + l_2} - 1\right). \tag{14}$$

Therefore the voltage within the grounded in both sides section HK varies, as we move from H to K, from an initial phasor value $R_{pg}\underline{I}_c$ to zero and finally to $-R_{pg}\underline{I}_c$.

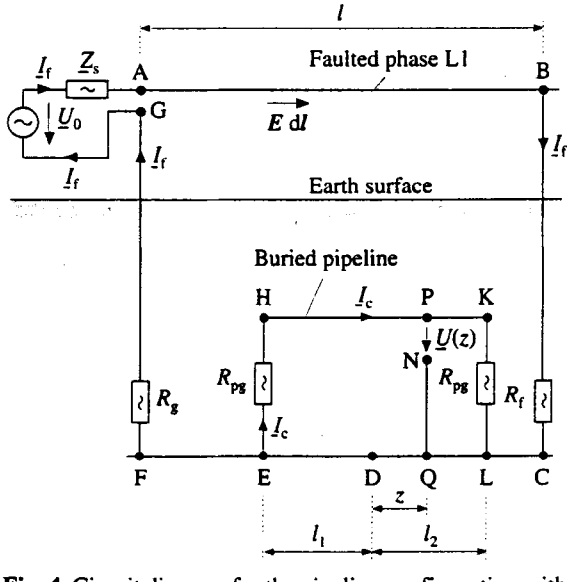

Fig. 4. Circuit diagram for the pipeline configuration with resistances R_{pg} at both end-points K and H

The corresponding magnitude variation will be from $|R_{pg}\underline{I}_c|$ to zero and finally to $|R_{pg}\underline{I}_c|$.

It should be mentioned that eq. (14) holds if the leakage currents are neglected, which is reasonable for nowadays synthetic coatings [16].

5 Results

The system shown in Fig. 1, 2 and 3 has been investigated for several different cases. According to eqs. (11a) and (11b), the fault current of phase L1 has been calculated equal to 2 000 A. Using this current, the two-dimensional diffusion equation has been solved for different separation distances d between the pipeline and the center of the overhead line, when initially no mitigation wires are present. Using FEM MVP results and applying *Faraday*'s law in the loop PNQDJP of Fig. 2 and 3, the voltage across points at pipeline sections HJ and KJ and remote earth is calculated. **Fig. 5** shows the amplitude of this voltage $U_{PN} = |\underline{U}_{PN}|$ for $\underline{I}_f = 1000\,\text{A} < 0°$ across a point P at a distance $z = 1\,000$ m from J and remote earth N, as well as its dependence on variations of separation distance d and of earth resistivity. This voltage is proportional to the fault current. Therefore, Fig. 5 can be easily used to predict the voltage for any value of current $\underline{I}_f$.

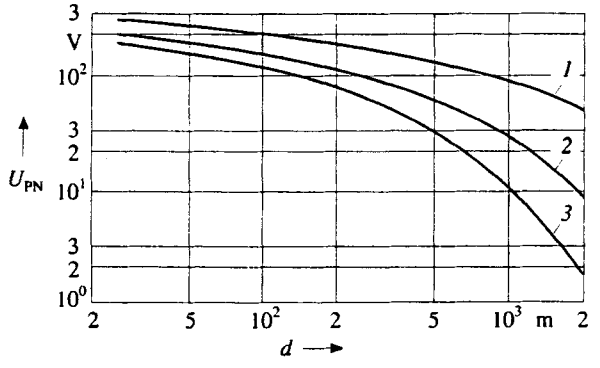

Fig. 5. Voltage U_{PN} for $\underline{I}_f = 1\,000\,\text{A} < 0°$ across the point P (at a distance $z = 1\,000$ m from J) and remote earth N of Fig. 2 and 3, as a function of the separation distance d of Fig. 1a (i. e. of the distance of the pipeline from the centre of the overhead line) for three different earth resistivities; curve *1* is for earth resistivity 1 000 Ωm, curve *2* for 100 Ωm and curve *3* for 30 Ωm

Number of mitigation wires / material	U_{PN} (in V) ($\underline{I}_f = 1\,000\,\text{A} < 0°$)
none	100.3
1 / copper	45
2 / copper	29.2
3 / copper	21.2
1 / aluminum	57
2 / aluminum	38
3 / aluminum	28.3

Tab. 1. Effect of the buried mitigation wires of Fig. 1a on magnetically induced voltage U_{PN}, across point P (at a distance $z = 1000$ m from J) of pipeline and remote earth N; the earth resistivity is 100 Ωm, the separation distance d between pipeline and the centre of the overhead line is 200 m, the bare mitigation wires have a radius equal to 5 mm and they are located at a distance equal to 1 m from the pipeline centre

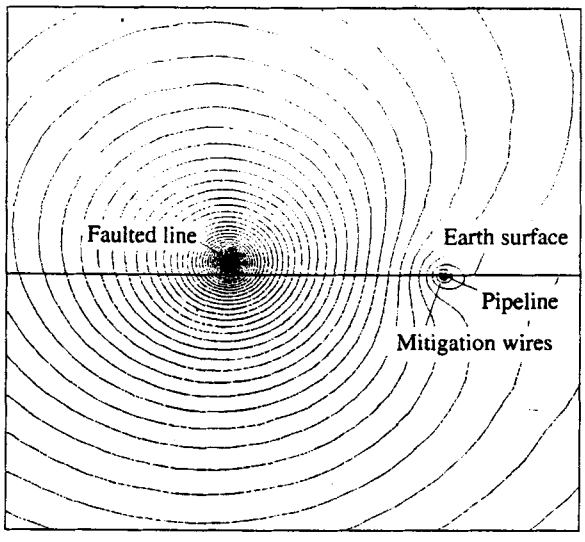

Fig 6. Flux lines (A = const) of the electromagnetic field, for a pipeline-overhead line separation distance equal to 200 m; there are three aluminum mitigation wires near the pipeline and the earth resistivity is 100 Ωm

The calculated voltages are exactly valid for a phase conductor height of 11 m. For separation distances $d > 50$ m the voltage differs less than 10 %, for conductor heights 8 m to 24 m. Consequently, the results presented here may also be used for other phase conductor heights.

Tab. 1 analyses the reduction of voltage obtained by installing progressively more bare mitigation wires with low resistivity material such as copper and aluminium, as shown in Fig. 1a. From the results of Tab. 1 it is clear that buried mitigation wires may be very effective. For example, the three aluminium mitigation wires reduce the pipeline voltage by 72.4 %. Using FEM it was found that, when the mitigation wire has a very low self impedance, the diameter of the conductor is much less important than the proximity of the wires to the pipeline and the number of wires used.

The effect of voltage mitigation due to the aluminium wires may be easily understood from the MVP distribution shown in **Fig. 6**. In this case there are three aluminium wires near to pipeline, as shown in the basic

Separation distance d (in m)	Technical Recommendation No 7 U_{PN} (in V)	FEM U_{PN} (in V)	Difference (in %)
25	223.7	202.1	9.65
70	169.2	155.1	8.33
100	146.15	136.2	6.8
200	107.7	100.3	6.87
500	60.5	55.1	8.92
800	38.2	35.1	8.11
1 000	28.9	26.4	8.65
2 000	8.46	7.82	7.56

Tab. 2. Comparison between Technical Recommendation No. 7 and FEM, concerning voltage U_{PN} for $\underline{I}_f = 1\,000\,\text{A} < 0°$ across point P (at a distance $z = 1\,000$ m from J) and remote earth N of Fig. 2 and 3, as a function of the separation distance d of Fig . 1a (i. e. of the distance of the pipeline from the centre of the overhead line) when no mitigation wires are present; the earth resistivity is 100 Ωm

system of Fig. 1a. The presence of the mitigation wires compressed the induction field towards the faulted line. On the other hand when no mitigation wires are present, the magnetic field has a y-axis symmetry and the flux lines in the pipeline region are similar to those on the left part of Fig. 6.

Finally, **Tab. 2** shows a comparison between FEM and Technical Recommendation No. 7 [6] results, for the same case shown in Fig. 2 and 3. This comparison concerns inductive voltage U_{PN} across points P (at a distance z = 1 000 m from J) and remote earth N of Fig. 2 and 3, as a function of the separation distance d of Fig. 1a (i. e. of the distance of the pipeline from the centre of the overhead line), when no mitigation wires are present. Since the difference is smaller than 10 %, the authors believe that FEM results are in good agreement with those provided by Technical Recommendation No. 7 [6].

6 Conclusions

The finite-element solution of the two-dimensional electromagnetic diffusion equation leads to useful conclusions concerning the inductive interaction between overhead transmission lines and buried conductors.

Using the distribution of the electromagnetic field (deriving from FEM solution) and *Faraday*'s law, fault current of the overhead transmission line as well as induced voltages in buried pipelines have been computed. The results concerning the voltage have been compared with corresponding results of Technical Recommendation No. 7 [6] and the differences found were less than 10 %. The influence of buried bare mitigation wires has also been investigated, leading in some cases to a pipeline voltage reduction up to 72.4 %. The method is also capable to take into account any configuration and number of overhead transmission lines, buried conductors and mitigation wires.

7 List of Principal Symbols, Subscripts, Superscripts and Abbreviations

7.1 Symbols

$\underline{Z}_s$	source impedance
R_f	fault resistance
R_g	ground resistance of source neutral
R_{pg}	pipeline-to-ground resistance
z	distance between a point P of pipeline and the nearest grounding of pipeline
$\underline{I}_f$	fault current
$\underline{A}_z$	z-direction component of magnetic vector potential
$\underline{J}_z$	z-direction component of total current density
σ	conductivity
ω	angular frequency
μ_0	vacuum permeability
μ_r	relative permeability
$\underline{J}_{sz}$	z-direction component of source current density
$\underline{I}_i$	current flowing through conductor i
S_i	cross section of conductor i
$\underline{J}_{ez}$	z-direction component of eddy current density
$\boldsymbol{B}$	magnetic flux density
$\boldsymbol{E}$	electric field intensity
l	conductor length
Φ	magnetic flux
$\underline{U}_0$	source phase voltage
$\underline{U}_{PN}$	voltage across point P of pipeline and remote earth N
$\underline{I}_c$	current flowing through the closed loop HKLQDEH
d	separation distance between the pipeline and the center of the overhead line

7.2 Superscripts

e	finite element e

7.3 Subscripts

e	eddy current
b	base quantity
i	conductor i

7.4 Abbreviations

EPRI	Electrical Power Research Institute
AGA	American Gas Association
ECCAPP	Electromagnetic & Conductive Coupling Analysis from Powerlines to Pipelines
FEM	Finite Element Method
MVP	Magnetic Vector Potential

References

[1] *Carson, J. R.:* Wave Propagation in Overhead Wires with Ground Return, Bell System. Tech. J. 5 (1926) no. 5, pp. 539–554

[2] *Pohl, J.:* Beeinflussung von umhüllten Rohrleitungen durch Hochspannungsfreileitungen. Cigré-Conf. 1966, Conf.-Rec. no. 326

[3] *Böcker, H.; Oeding, D.:* Induktionsspannung an Pipelines in Trassen von Hochspannungsleitungen. Elektriz.-wirtsch. 65 (1966) no. 5, pp. 157–170

[4] *Kaiser, G.:* Die elektrischen Konstanten von Rohrleitungen und ihre Messung. ETZ-A Elektrotech. Z. 87 (1966) no. 2, pp. 792–796

[5] *Sunde, E. D.:* Earth Conduction Effects in Transmission Systems. New York/USA: Dover Publ., 1968

[6] Tech. Recomm. No. 7: Arbitration Agency for Problems of Interference Between Installations of the German Federal Railways, the German Federal Post Office and the Association of German Power Utilities. Frankfurt a. M. /Germany: Verlags und Wirtsch.-gesellsch. der Elektrizitätswerke mbH (VWEW), 1982

[7] *Dabkowski, J.; Taflove, A.:* Mutual Design Considerations for Overhead AC Transmission Lines and Gas Transmission Pipelines. Palo Alto, CA/USA: EPRI Rep. EL-904, 1978, vol. 1, Ch. 3

[8] *Fraiser et al.:* Power Line-Induced AC Potential on Natural Gas Pipelines for Complex Rights-of-Way Configurations. Palo Alto, CA/USA: EPRI/A.G.A. Project 742-2 EL-3106/PR-151-127, 1983

[9] Power Line Fault Current Coupling to Nearby Natural Gas Pipelines. Palo Alto, CA/USA: EPRI/A.G.A. Project 742 EL-5472/PR176-510, 1987

[10] *Dawalibi, F.; Southey, R. D.:* Analysis of Electrical Interference from Power Lines to Gas Pipelines Part I: Computation Methods. IEEE Trans. on Power Delivery PWRD-4 (1989) no. 3, pp. 1 840–1 846

[11] *Dawalibi, F.; Southey, R. D.:* Analysis of Electrical Interference from Power Lines to Gas Pipelines, Part II: Parametric Analysis. IEEE Trans. on Power Delivery PWRD-5 (1990) no. 1, pp. 415–421
[12] *Pollaczeck, F.:* On the Field Produced by an Infinitely Long Wire Carrying Alternating Current. Electr. Nachr. Tech. 3 (1931) no. 9, pp. 339–359
[13] *Kouteynikoff, P.:* Résultats d' une enquete internationale sur les règles limitant les perturbations créés sur les canalisations par les ouvrages électriques à haute tension. Electra (1987) no. 110, pp. 55–66
[14] *Meynaud, P.:* Progress Report of Study Committee 36 (Interference) for 1990 and 1991. Electra no. 142, 1992, pp. 89–95
[15] Cigré WG 36.02: Guide relatif á l' influence des installations électriques á haute tension sur les canalisations métalliques (á paraitre). Paris/France: Cigré
[16] *Jacquet, B.; Kouteynikoff, P.:* Influence of High Voltage Lines and Installations on Metal Pipelines. Paris/France: Cigré Pap. 36-203 (presented in the name of Study Committee 36), 1990
[17] Cigré WG 36.02: Guide Concerning Influence of High Voltage AC Power Systems on Metallic Pipelines. Paris/France: Prelim. Guide 36-92 (WG02) 17, 1992
[18] *Labridis, D.; Dokopoulos, P.:* Finite element computation of field, losses and forces in a three-phase gas cable with non-symmetrical conductor arrangement. IEEE Trans. on Power Delivery PWDR-3 (1988) no. 4, pp. 1326–1333
[19] *Weiss, J.; Csendes, Z.:* A one-step finite element method for multiconductor skin effect problems. IEEE Trans. on Power Appar. a. Syst. PAS-101 (1982) no. 10, pp. 3796–3803
[20] *Cendes, Z.; Shenton, D.; Shahnasser, H.:* Magnetic field computation using Delaunay triangulation and complementary finite element methods. IEEE Trans. on Magn. MAG-19 (1983) no. 6, pp. 2551–2554
[21] *Labridis, D. P.:* Comparative presentation of criteria used for adaptive finite element mesh generation in multiconductor eddy current problems. Submitted for publication in IEEE Trans. on Magn.

Manuscript received on May 14, 1996

The Authors

Kostas J. Satsios (1971) received the Dipl.-Eng. degree from the Department of Electrical Engineering at the Aristotle University of Thessaloniki /Greece in 1994. Since 1994 he is a Ph.D. student in the Department of Electrical and Computer Engineering at the Aristotle University of Thessaloniki. His research interests are in finite elements and artificial-intelligence applications in power systems. He is a member of the Society of Professional Engineers of Greece. (Aristotle University of Thessaloniki, Department of Electrical and Computer Engineering, Power Systems Laboratory, P.O. Box 486, GR-54006 Thessaloniki/Greece, Phone: +30 31/99 63 56, Fax: +30 31/99 63 02, E-mail: satsios@eng.auth.gr)

Dimitris P. Labridis (1958) received the Dipl.-Eng. degree and the Ph.D. degree from the Department of Electrical Engineering at the Aristotle University of Thessaloniki/Greece in 1981 and 1989, respectively. From 1982 to 1993 he has been working, at first as a Research Assistant and later as a Lecturer, at the Department of Electrical Engineering at the Aristotle University of Thessaloniki. Since 1994 he has been an Assistant Professor at the same Department. His special interests are power-system analysis with special emphasis on the simulation of transmission and distribution systems, electromagnetic and thermal field analysis and numerical methods in engineering. (Aristotle University of Thessaloniki, Department of Electrical and Computer Engineering, Power Systems Laboratory, P.O. Box 486, GR-54006 Thessaloniki/Greece, Phone: +30 31/99 63 74, Fax: +30 31/99 63 02, E-mail: labridis @eng.auth.gr)

Petros S. Dokopoulos (1939) received the Dipl.-Eng. degree from the Technical University of Athens/Greece in 1962 and the Ph.D. degree from the University of Brunswick/Germany, in 1967. From 1962 to 1967 he was with the Laboratory for High Voltage and Transmission at the University of Brunswick, from 1967 to 1974 with the Nuclear Research Centre at Julich/Germany, and from 1974 to 1978 with the Joint European Torus. Since 1978 he has been Full Professor at the Department of Electrical Engineering at the Aristotle University of Thessaloniki. He has worked as consultant to Brown Boveri & Cie, Mannheim/Germany, to Siemens, Erlangen/ Germany, to Public Power Corporation/-Greece and to National Telecommunication Organization and construction companies in Greece. His scientific fields of interest are dielectrics, power switches, power generation (conventional and fusion), transmission, distribution and control in power systems. (Aristotle University of Thessaloniki, Department of Electrical and Computer Engineering, Power Systems Laboratory, P.O. Box 486, GR-54006 Thessaloniki, Greece, Phone: +30 31/99 63 21, Fax: +30 31/99 63 02, E-mail: dokopoulos@eng.auth.gr)